Integration of higher-order dynamic fields into MR image reconstruction

B. J. Wilm[1], C. Barmet[1], M. Pavan[1], P. Boesiger[1], and K. P. Pruessmann[1]

[1]Institute for Biomedical Engineering, University and ETH Zurich, Zurich, Zurich, Switzerland

Introduction

Conventional magnetic resonance imaging uses linear gradient fields for spatial encoding, allowing the use of Fourier based reconstruction methods. The incorporation of dynamic non-linear phase terms into reconstruction is uncommon, as its evolution during the readout is usually unknown and reconstruction techniques have so far not been available. Recent improvements in magnetic field monitoring opened up the possibility of capturing higher-order dynamic field evolution, providing the necessary information to correct for the image distortions they cause. The present work introduces a technique for higher order field reconstruction based on monitored higher order phase evolution.

The method is applied to phantom and in-vivo diffusion weighted EPI. Diffusion imaging is a particularly challenging application, since parametric maps are calculated from sets of variably diffusion weighted (DW) images. Hence the geometrical congruence between different images is of utmost importance but hampered by strong eddy current induced magnetic field perturbations during the data readout, varying with the diffusion encoding.

Methods

2D single-shot spin-echo EPI data (TE=80ms, TR=5000ms, 76 phase encodes, readout duration=45.8ms, FOV=230mm) was acquired in a coronal (in-vitro) and a transverse (in-vivo) plane. Diffusion weighting (b=1000 mm^2/s) was applied in the frequency-encoding, phase-encoding and slice-selection direction; additionally non-DW (b_0) reference data was acquired. To facilitate in-vitro data analysis a spherical phantom filled with low-diffusive silicon oil was employed. All imaging scans were performed on a 3T Philips Achieva system using an 8-channel head coil. Subsequently the imaging object and coil were removed and replaced by an array of 16 NMR probes [1] uniformly distributed on the surface of a sphere with a diameter of 20 cm. The scans were repeated, acquiring the phase data from the 16 probes which allows for (least-squares) fitting of the higher-spatial-order phase model [2] to

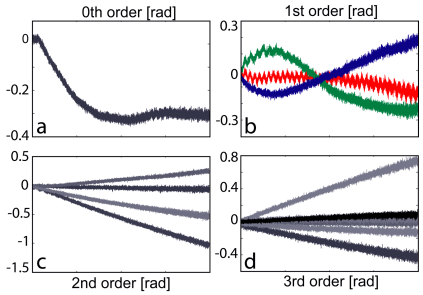

Fig 1: Maximum phase effect in the imaging volume during the EPI readout caused by eddy-current-induced phase terms: a) global phase b) k_x(red), k_y(green), k_z(blue), c,d): higher-order terms

$$\varphi_p(\mathbf{t}) = \sum_m k_m(\mathbf{t}) b_m(\mathbf{r}_p),$$

where φ_p is the signal phase of the p-th probe, demodulated by its static reference frequency and unwrapped. k_m denotes the m-th phase coefficient with the basis functions b_m defining the spatial phase expansion and r_p denoting the probe's position. Here the basis b is formed by the first 16 real-valued spherical harmonics (Tab. 1), covering the 0th to 3rd spatial order. For image reconstruction the generalized phase evolution was incorporated in a net encoding matrix

$$E_{\kappa,\rho} = \exp(i \sum_m k_m(\mathbf{t}_\kappa) b_m(\mathbf{r}_\rho)),$$

where κ,ρ count the sampling time points and pixels of the target image, respectively. Individual coil images were then obtained by iteratively solving [3] the normal equation of the forward signal model,

$$E^H E\, I(\mathbf{r}_\rho) = E^H s(\mathbf{t}_\kappa),$$

$s(t_\kappa)$ denoting the signals acquired with the respective coil. Due to the size of E and E^H their values were calculated on demand rather than stored in memory. The quality of geometric congruence was assessed by absolute difference images between DW images and the b_0 image (where the images were normalized to have identical mean values); additionally the maximum relative difference ($diff_{max}$) of these image pairs was evaluated. To appreciate the benefit of this method, the images were compared to the standard image reconstruction of the system, with and without image co-registration [4]), as well as to probes-driven reconstruction with only a first-order spatial phase expansion.

Tab.1: spherical harmonics

nr.	basis function b_m
0	1
1	x
2	y
3	z
4	xy
5	zy
6	$3z^2 - (x^2 + y^2 + z^2)$
7	xz
8	$x^2 - y^2$
9	$3x^2y - y^3$
10	xyz
11	$y\,(5z^2 - (x^2 + y^2 + z^2))$
12	$5z^3 - 3z\,(x^2 + y^2 + z^2)$
13	$x\,(5z^2 - (x^2 + y^2 + z^2))$
14	$x^2z - y^2z$
15	$x^3 - 3xy^2$

Results

Significant field perturbations of 2nd and 3rd order are introduced by the DW gradients (Fig. 1). Correspondingly, reconstruction with the full 3rd-order phase model yielded the least distorted DW phantom image, as reflected by the smallest difference from its non-DW counterpart (Fig. 2d). Elevated differences were observed with the alternative reconstruction options (2a-c). Similarly, in-vivo images, obtained with probes-driven higher-order reconstruction, showed no visible distortion for any of the DW directions (Fig. 3a-c), relative to the b_0 image (Fig. 3d). The resulting geometric congruence permitted straightforward calculation of derived parameters such as the apparent diffusion coefficient (ADC) (Fig. 3f).

Discussion and Conclusion

The present work introduces image reconstruction based on higher-order spatial expansion of the phase evolution in the sample. It has been found that eddy currents of diffusion gradients can induce considerable higher-order field perturbations, causing residual error in conventional first-order reconstruction. Higher-order reconstruction largely eliminated these errors in phantom experiments, outperforming a commonly applied co-registration method. In the present work the phase expansion was obtained by separate field probe measurements, relying on reproducibility of the eddy current effects. Provided sufficiently many receiver channels higher- order field monitoring could also be performed simultaneously with the actual image acquisition [2] to save scan time and correct for longer-term effects such as field drifts caused by gradient heating. DW imaging has been used as a challenging test case for the higher-order approach. However, it can be applied equally to other MRI or MR spectroscopy techniques. It can also be readily extended by static B_0 correction to achieve yet greater geometrical fidelity and by parallel imaging or partial Fourier encoding to reduce TE and T_2* effects.

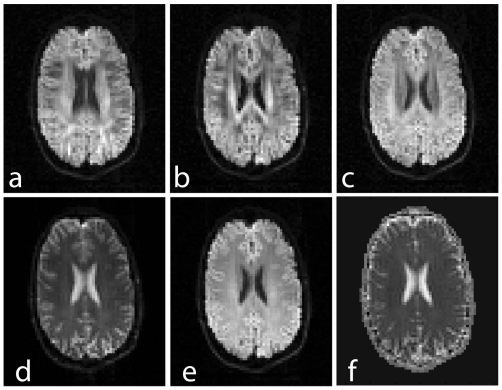

Fig. 3: a) DW_{read},b) DW_{phase},c) DW_{slice},d) b_0 e) mean of a-c, f) mean ADC

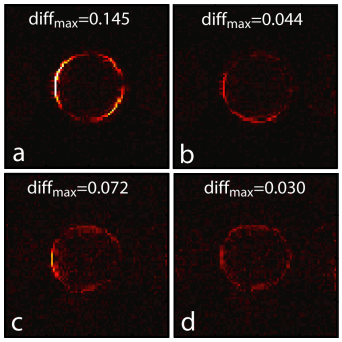

Fig.2: Relative difference between the b_0 and DW image of a phantom, obtained with a) standard reconstruction, b) same + co-registration, c) 1st-order phase model, d) 3rd-order phase model. DW was applied in the phase-encoding direction.

References

1: De Zanche N et al., 2008, MRM. 2008 60(1):176-86,

2: Barmet C et al., 2008, MRM 60(1):187-97,

3: Pruessmann KP, 2001, MRM 46:638-651,

4: Netsch et al., 2004 IEEE trans. medical imaging, 23(7):789-798.